Chapter 11 | Thermally Stratified Surface Layer

11.1 The Monin–Obukhov Similarity Theory

In the previous chapter, we showed that the atmospheric surface layer under neutral conditions is characterized by a logarithmic wind profile and nearly uniform (with respect to height) profiles of momentum flux and standard deviations of turbulent velocity fluctuations. It was also mentioned that the neutral stability condition is an exception rather than the rule in the lower atmosphere. More often, the turbulent exchange of heat between the surface and the atmosphere leads to thermal stratification of the surface layer and, to some extent, of the whole PBL, as shown in Chapter 5. It has been of considerable interest to micrometeorologists to find a suitable theoretical or semiempirical framework for a quantitative description of the mean and turbulence structure of the stratified surface layer. The Monin–Obukhov similarity theory has provided the most suitable and acceptable framework for organizing and presenting micrometeorological data, as well as for extrapolating and predicting certain micrometeorological information where direct measurements are not available.

11.1.1 The similarity hypothesis

The basic similarity hypothesis first proposed by Monin and Obukhov (1954) is that in a horizontally homogeneous surface layer the mean flow and turbulence characteristics depend only on the four independent variables: the height above the surface z, the surface drag τ_0/ρ, the surface kinematic heat flux $H_0/\rho c_p$, and the buoyancy variable g/T_0 (this appears in the expressions for buoyant acceleration and static stability given earlier). This is an extension of the earlier hypothesis for the neutral surface layer. The simplifying assumptions implied in this similarity hypothesis are that the flow is horizontally homogeneous and quasistationary, the turbulent fluxes of momentum and heat are constant (independent of height), the molecular exchanges are insignificant in comparison with turbulent exchanges, the rotational effects can be ignored in the

surface layer, and the influence of surface roughness, boundary layer height, and geostrophic winds is fully accounted for through τ_0/ρ.

Because the four independent variables in the M–O similarity hypothesis involve three fundamental dimensions (length, time, and temperature), according to Buckingham's theorem, one can formulate only one independent dimensionless combination out of them. The combination traditionally chosen in the Monin–Obukhov similarity theory is the buoyancy parameter

$$\zeta = z/L$$

where

$$L = -u_*^3/[k(g/T_0)(H_0/\rho c_p)] \tag{11.1}$$

is an important buoyancy length scale, known as the Obukhov length after its originator. In his 1946 article in an obscure Russian journal (for the English translation, see Obukhov, 1946/1971), Obukhov introduced L as 'the characteristic height (scale) of the sublayer of dynamic turbulence'; he also generalized the semiempirical theory of turbulence to the stratified atmospheric surface layer and used this approach to describe theoretically the mean wind and temperature profiles in the surface layer in terms of the fundamental stability parameter z/L.

One may wonder about the physical significance of the Obukhov length (L) and the possible range of its values. From the definition, it is clear that the values of L may range from $-\infty$ to ∞, the extreme values corresponding to the limits of the heat flux approaching zero from the positive (unstable) and the negative (stable) side, respectively. A more practical range of $|L|$, corresponding to fairly wide ranges of values of u_* and $|H_0|$ encountered in the atmosphere, is shown in Figure 11.1. Here, we have assumed a typical value of $kg/T_0 = 0.013\ \mathrm{m\ s^{-2}\ K^{-1}}$, which may not differ from the actual value of this by more than 15%. In magnitude $|L|$ represents the thickness of the layer of dynamic influence near the surface in which shear or friction effects are always important. The wind shear effects usually dominate and the buoyancy effects essentially remain insignificant in the lowest layer close to the surface ($z \ll |L|$). On the other hand, buoyancy effects may dominate over shear-generated turbulence for $z \gg |L|$. Thus, the ratio z/L is an important parameter measuring the relative importance of buoyancy versus shear effects in the stratified surface layer, similar to the Richardson number (Ri) introduced earlier. The negative sign in the definition of L is introduced so that the ratio z/L has the same sign as Ri. Later on, it will be shown that Ri and z/L are intimately related to each other, even though they have different distributions with respect to height in the surface layer (z/L obviously varies linearly with height, showing the increasing importance of buoyancy with height above the surface).

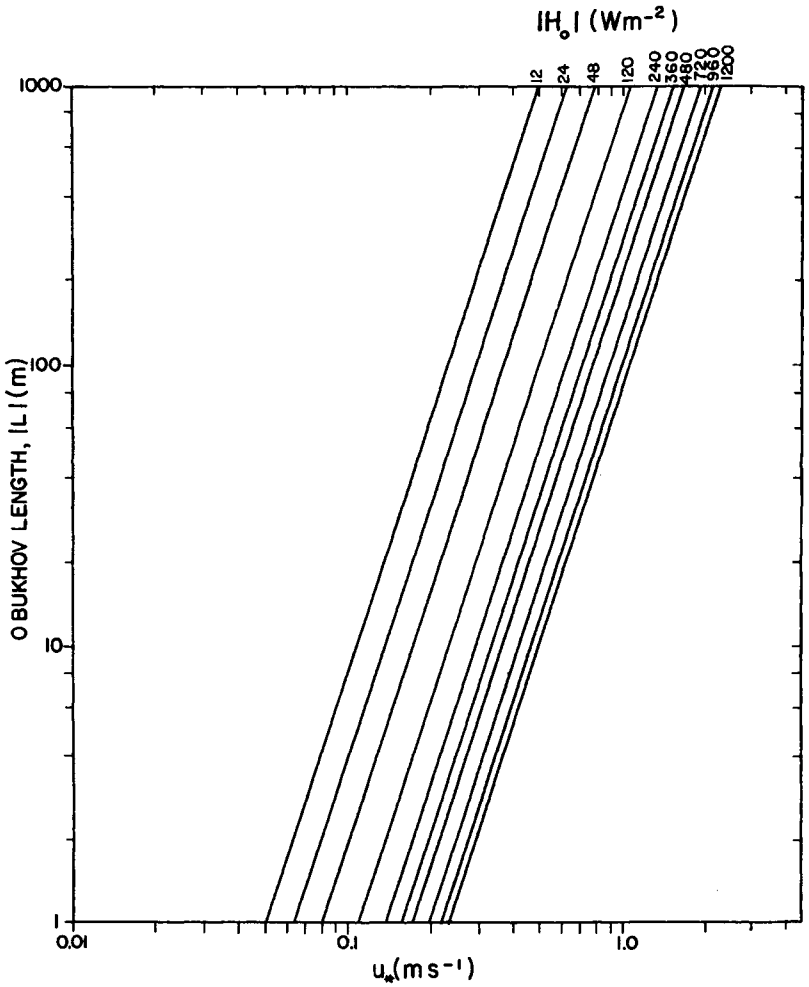

Figure 11.1 Obukhov's buoyancy length as a function of the friction velocity and the surface heat flux.

11.1.2 The M–O similarity relations

The following characteristic scales of length, velocity, and temperature are used to form dimensionless groups in the Monin–Obukhov similarity theory:

Length scales:	z and L
Velocity scale:	u_*
Temperature scale:	$\theta_* = -H_0/\rho c_p u_*$

The similarity prediction that follows from the M–O hypothesis is that any mean flow or average turbulence quantity in the surface layer, when normalized by an appropriate combination of the above-mentioned scales, must be a unique function of z/L only. Thus, a number of similarity relations can be written for the various quantities (dependent variables) of interest. For example, with the x axis oriented parallel to the surface stress or wind (the appropriate surface layer coordinate system), the dimensionless wind shear and potential temperature gradient are usually expressed as

$$\begin{aligned}(kz/u_*)(\partial U/\partial z) &= \phi_m(\zeta)\\ (kz/\theta_*)(\partial \Theta/\partial z) &= \phi_h(\zeta)\end{aligned} \tag{11.2}$$

in which the von Karman constant k is introduced only for the sake of convenience, so that $\phi_m(0) = 1$, and $\phi_m(\zeta)$ and $\phi_h(\zeta)$ are the basic universal similarity functions which relate the constant fluxes

$$\begin{aligned}\tau &= \tau_0 = \rho u_*^2\\ H &= H_0 = -\rho c_p u_* \theta_*\end{aligned} \tag{11.3}$$

to the mean gradients in the surface layer.

It is easy to show from the definition of Richardson number and Equations (11.1)–(11.2) that

$$\mathrm{Ri} = \zeta \phi_h(\zeta)/\phi_m^2(\zeta) \tag{11.4}$$

which relates Ri to the basic stability parameter $\zeta = z/L$ of the M–O similarity theory. The inverse of Equation (11.4), namely, $\zeta = f(\mathrm{Ri})$ is often used to determine ζ and, hence, the Obukhov length L from easily measured gradients of velocity and temperature at one or more heights in the surface layer. Then, Equations (11.2) and (11.3) can be used to determine the fluxes of momentum and heat, knowing the empirical forms of the similarity functions $\phi_m(\zeta)$ and $\phi_h(\zeta)$ from carefully conducted experiments.

Other properties of flow which relate turbulent fluxes to the local mean gradients, such as the exchange coefficients of momentum and heat and the corresponding mixing lengths, can also be expressed in terms of $\phi_m(\zeta)$ and $\phi_h(\zeta)$. For example, it is easy to show that

$$\begin{aligned}K_m/(kzu_*) &= \phi_m^{-1}(\zeta)\\ K_h/(kzu_*) &= \phi_h^{-1}(\zeta)\\ K_h/K_m &= \phi_m(\zeta)/\phi_h(\zeta)\end{aligned} \tag{11.5}$$

which can be used to prescribe the eddy diffusivities or their ratio K_h/K_m in the stratified surface layer.

11.2 Empirical Forms of Similarity Functions

As mentioned earlier, a similarity theory based on a particular similarity hypothesis and dimensional analysis can only suggest plausible functional relationships between certain dimensionless parameters. It does not tell anything about the forms of those functions, which must be determined empirically from accurate observations during experiments specifically designed for this purpose. Experimental verification is also required, of course, for the original similarity hypothesis or its consequences (e.g., predicted similarity relations).

Following the proposed similarity theory by Monin and Obukhov (1954), a number of micrometeorological experiments have been conducted at different locations (ideally, flat and homogeneous terrain with uniform and low roughness elements) and under fair-weather conditions (to satisfy the conditions of quasistationarity and horizontal homogeneity) for the expressed purpose of verifying the M–O similarity theory and for accurately determining the forms of the various similarity functions. Early experiments lacked direct and accurate measurements of turbulent fluxes, which could be estimated only after making some *a priori* assumptions about flux-profile relations. The 1953 Great Plains Experiment at O'Neill, Nebraska, was one of the earliest concerted efforts in observing the PBL in which micrometeorological measurements were made by several different groups, using different instrumentation and techniques (Lettau and Davidson, 1957). But, here too, as in subsequent Australian and Russian experiments in the 1960s, the flux measurements suffered from severe instrument-response problems and were not very reliable. Still, these experiments could verify the general validity of M–O similarity theory and give the approximate forms of the similarity functions $\phi_m(\zeta)$ and $\phi_h(\zeta)$. Empirical evaluations of the M–O similarity functions based on several micrometeorological experiments conducted in southern Australia have been reported by Dyer (1967), Dyer and Hicks (1970), Webb (1970), and Hicks (1976). Garratt and Hicks (1990) presented an overview of these experiments and their results.

Perhaps the best micrometeorological experiment conducted so far, for the specific purpose of determining the M–O similarity functions, was the 1968 Kansas Field Program (Izumi, 1971). A 32 m tower located in the center of a 1 mile^2 field of wheat stubble ($h_0 \approx 0.18$ m) was instrumented with fast-response cup anemometers, thermistors, resistance thermometers, and three-dimensional sonic anemometers at various levels. These were used to determine mean velocity and temperature gradients, as well as the momentum and heat fluxes using the eddy correlation method. In addition, two large drag plates installed

nearby were used to measure the surface stress directly. Both heat and momentum fluxes were found to be constant with height, within the limits of experimental accuracy ($\pm 20\%$, for fluxes). The flux-profile relations derived from the Kansas Experiment are discussed in detail by Businger *et al.* (1971).

The generally accepted forms of $\phi_m(\zeta)$ and $\phi_h(\zeta)$ on the basis of the various micrometeorological experiments are

$$\phi_m = \begin{cases} (1 - \gamma_1 \zeta)^{-1/4} & \text{for } \zeta < 0 \text{ (unstable)} \\ 1 + \beta_1 \zeta, & \text{for } \zeta \geq 0 \text{ (stable)} \end{cases} \tag{11.6}$$

$$\phi_h = \begin{cases} \alpha(1 - \gamma_2 \zeta)^{-1/2} & \text{for } \zeta < 0 \text{ (unstable)} \\ \alpha + \beta_2 \zeta, & \text{for } \zeta \geq 0 \text{ (stable)} \end{cases} \tag{11.7}$$

There remain some differences, however, in the estimated values of the constants, α, β_1, β_2, γ_1, and γ_2 in the above expressions as obtained by different investigators. The main causes of these differences are the unavoidable measurement errors and deviations from the ideal conditions assumed in the theory (Yaglom, 1977; Hogstrom, 1988). The originally estimated values from the Kansas Experiment were (Businger *et al.*, 1971):

$$\alpha = 0.74; \quad \beta_1 = \beta_2 = 4.7; \quad \gamma_1 = 15; \quad \gamma_2 = 9 \tag{11.8}$$

The corresponding formulas [Equations (11.6) and (11.7) for ϕ_m and ϕ_h with the above empirical values of constants are shown in Figures 11.2 and 11.3 together with the observed Kansas data. These data are characterized by relatively small scatter, compared with other micrometeorological data sets used for evaluating the M–O similarity functions (Hogstrom, 1988). Still, they were probably subjected to significant errors due to distortion of air flow around instrument boxes mounted on the tower. In particular, unusually low values of $k = 0.35$ and $\alpha = 0.74$, estimated from the Kansas data, have been attributed to likely flow distortion errors. The low value of the von Karman constant, compared to its traditional value of 0.40, generated some controversial hypotheses or explanations on the possible dependence of k on roughness Reynolds number. But more definitive experimental determinations of the same in the 1980s did not find any such dependence and have confirmed its traditional value (Hogstrom, 1988). More accurate estimates of α from both the field and laboratory experiments have also indicated that α may not be significantly different from one (Hogstrom, 1988). Still, the precise forms of the M–O similarity functions $\phi_m(\zeta)$ and $\phi_h(\zeta)$ remain far from being settled (Hogstrom, 1996).

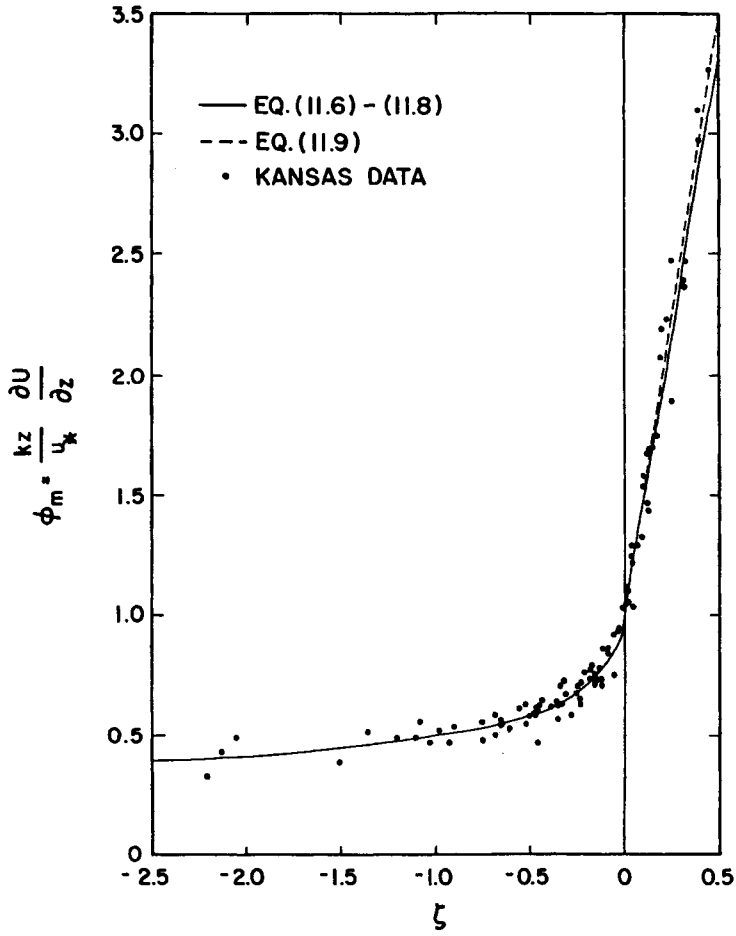

Figure 11.2 Dimensionless wind shear as a function of the M–O stability parameters. [Kansas data from Izumi (1971).]

In view of the above-mentioned uncertainties in measurements and in the determination of empirical similarity functions or constants, the following simpler flux-profile relations can be recommended for most practical applications in which great precision is not warranted:

$$\begin{aligned} \phi_h = \phi_m^2 &= (1 - 15\zeta)^{-1/2}, \quad \text{for } \zeta < 0 \\ \phi_h = \phi_m &= 1 + 5\zeta, \qquad\quad \text{for } \zeta \geq 0 \end{aligned} \tag{11.9}$$

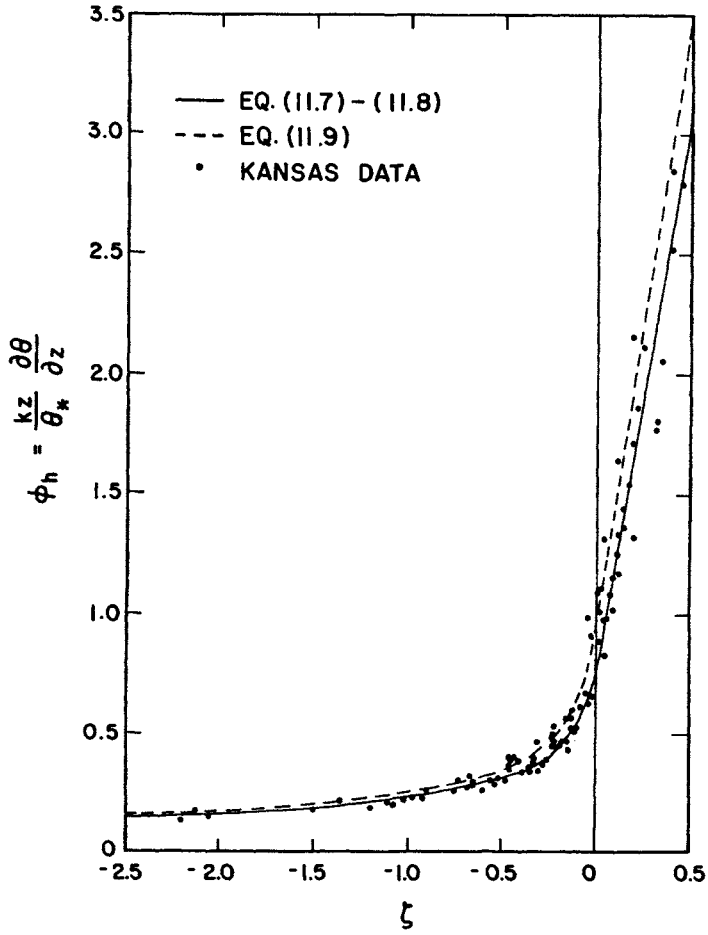

Figure 11.3 Dimensionless potential temperature gradient as a function of the M–O stability parameters. [Kansas data from Izumi (1971).]

These deviate from the Kansas relations [Equations (11.6)–(11.8)] only slightly, but have the advantage of relating ζ to Ri more simply and explicitly as

$$\begin{aligned} \zeta &= \mathrm{Ri}, && \text{for } \mathrm{Ri} < 0 \\ \zeta &= \frac{\mathrm{Ri}}{1 - 5\mathrm{Ri}}, && \text{for } 0 \leq \mathrm{Ri} \leq 0.2 \end{aligned} \tag{11.10}$$

These are verified against the Kansas data in Figure 11.4.

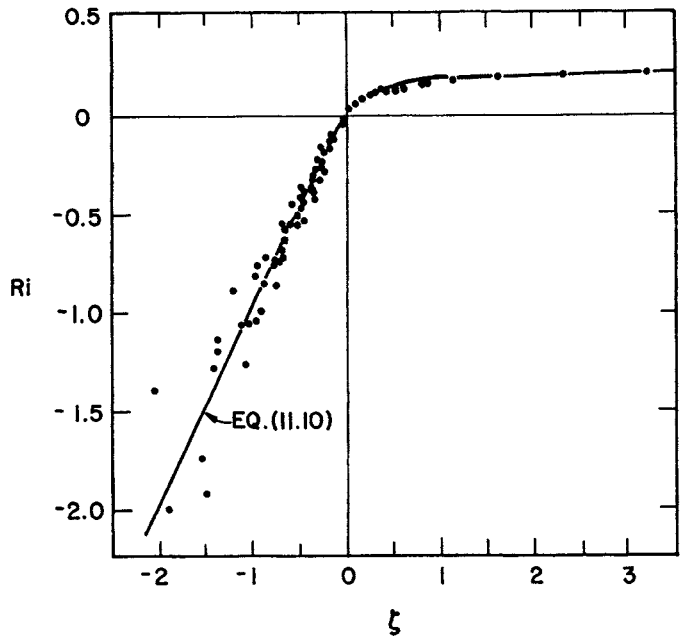

Figure 11.4 The Richardson number as a function of the M–O stability parameters. Equation (11.10) (—) is compared with Kansas data. [After Businger *et al.* (1971).]

After substituting from Equations (11.9) and (11.10) into Equation (11.5), the eddy diffusivities of heat and momentum can also be expressed as functions of the Richardson number

$$\begin{aligned} \frac{K_m}{kzu_*} &= \begin{cases} (1 - 15\mathrm{Ri})^{1/4}, & \text{for } \mathrm{Ri} < 0 \\ 1 - 5\mathrm{Ri}, & \text{for } 0 \leq \mathrm{Ri} \leq 0.2 \end{cases} \\ \frac{K_h}{kzu_*} &= \begin{cases} (1 - 15\mathrm{Ri})^{1/2} & \text{for } \mathrm{Ri} < 0 \\ 1 - 5\mathrm{Ri}, & \text{for } 0 \leq \mathrm{Ri} \leq 0.2 \end{cases} \end{aligned} \tag{11.11}$$

These are represented in Figure 11.5. Note that the eddy diffusivities of heat and momentum are equal under stably stratified conditions; they decrease rapidly with increasing stability and vanish as the Richardson number approaches its critical value of $\mathrm{Ri}_c = 1/\beta \cong 0.2$.

There is a question about the validity of the above-mentioned empirically estimated similarity functions under extremely unstable (approaching free convection) and extremely stable (approaching critical Ri) conditions.

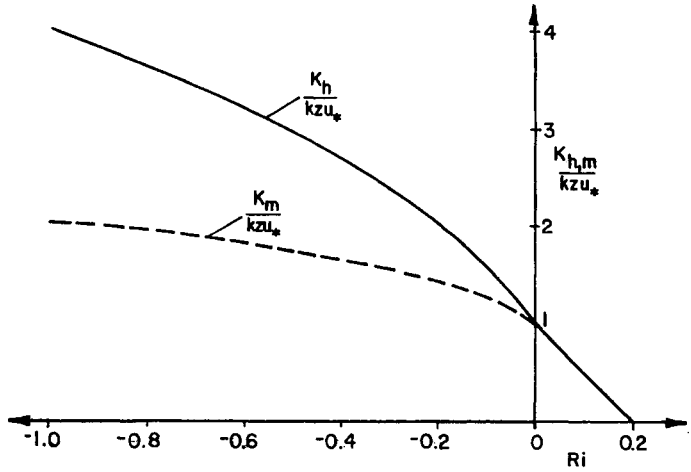

Figure 11.5 Variation of the dimensionless eddy diffusivities of heat and momentum with Richardson number according to Equations (11.11).

Micrometeorological data used in the determination of the above M–O similarity functions have generally been limited to the moderate stability range of $-5 < \zeta < 2$, and, as such, are strictly valid in this range. As a matter of fact, in conditions approaching free convection ($-\zeta \gg 1$, or $\zeta \to -\infty$), the above expressions for ϕ_h and K_h are not quite consistent with the local free convection similarity relations for $\partial\Theta/\partial z$ and K_h derived in Chapter 9. In order for them to be consistent one must have $\phi_h \sim (-\zeta)^{-1/3}$ for $-\zeta \gg 1$. Some of the proposed forms of ϕ_h satisfy this condition, but do not represent the data well, especially for $-\zeta < 2$.

On the other side of strong stability conditions, there is some evidence of a linear velocity profile in the lower part of the PBL, including the surface layer, which appears to be consistent with the M–O relation for $\phi_m(\zeta)$ for $\zeta \gg 1$. There is also other experimental evidence suggesting the limiting value of $\zeta \cong 1$ for the validity of the M–O relation $\phi_m = 1 + \beta\zeta$ (Webb, 1970; Hicks, 1976). In any case, strong stability conditions usually occur at nighttime under clear skies and weak winds. Because the temperature profile under such conditions is strongly influenced by longwave atmospheric radiation, which is ignored in the M–O similarity theory, the temperature field may not follow the M–O similarity. Experimental estimates of both $\phi_m(\zeta)$ and $\phi_h(\zeta)$ indicate that these functions become increasingly flatter as ζ increases above 0.5 (Hicks, 1976; Holtslag, 1984).

11.3 Wind and Temperature Profiles

Integration of Equations (11.2) with respect to height yields the velocity and potential temperature profiles in the form

$$\begin{aligned} U/u_* &= (1/k)[\ln(z/z_0) - \psi_m(z/L)] \\ (\Theta - \Theta_0)/\theta_* &= (1/k)[\ln(z/z_0) - \psi_h(z/L)] \end{aligned} \tag{11.12}$$

in which Θ_0 is the extrapolated temperature at $z = z_0$ and ψ_m and ψ_h are different similarity functions related to ϕ_m and ϕ_h, respectively, as

$$\begin{aligned} \psi_m\left(\frac{z}{L}\right) &= \int_{z_0/L}^{z/L} [1 - \phi_m(\zeta)] \frac{d\zeta}{\zeta} \\ \psi_h\left(\frac{z}{L}\right) &= \int_{z_0/L}^{z/L} [1 - \phi_h(\zeta)] \frac{d\zeta}{\zeta} \end{aligned} \tag{11.13}$$

For smooth and moderately rough surfaces, z_0/L is usually quite small and the integrands in Equation (11.13) are well behaved at small ζ, so that the lower limit of integration can essentially be replaced by zero. With this approximation, the ψ functions can be determined for any appropriate forms of ϕ functions. For example, corresponding to Equation (11.9), we obtain

$$\begin{aligned} \psi_m &= \psi_h = -5\frac{z}{L}, \quad \text{for } \frac{z}{L} \geq 0 \\ \psi_m &= \ln\left[\left(\frac{1+x^2}{2}\right)\left(\frac{1+x}{2}\right)^2\right] - 2\tan^{-1} x + \frac{\pi}{2}, \quad \text{for } \frac{z}{L} < 0 \\ \psi_h &= 2\ln\left(\frac{1+x^2}{2}\right), \quad \text{for } \frac{z}{L} < 0 \end{aligned} \tag{11.14}$$

where $x = (1 - 15z/L)^{1/4}$.

Note that the deviations in profiles from the log law increase with increasing magnitude of z/L. Under stable conditions the profiles are log linear and tend to become linear for large values of z/L.

Under unstable conditions ($\zeta < 0$), on the other hand, ψ_m and ψ_h are positive, so that the deviations from the log law are of opposite sign (negative). Consequently, the velocity and temperature profiles in the surface layer are expected to become more and more curvilinear as instability increases. The observed winds and temperatures are usually plotted against $\log z$ or $\ln z$, instead of a linear height scale, in order to reduce the profile curvature and to

clearly show their deviations from the log law due to buoyancy effects in the surface layer.

If the wind profile in the stratified surface layer is represented by the power-law relation (10.2), as is often done in air pollution/dispersion models, the exponent m can be specified as a function of surface roughness and stability as

$$m = \phi_m(\zeta_r)/[\ln(z_r/z_0) - \psi_m(\zeta_r)] \tag{11.15}$$

where $\zeta_r = z_r/L$ and the reference height z_r is of the order of 10 m, so that it falls within the constant flux surface layer. Comparing the above expression for m with Equation (10.8) for neutral stability, it is obvious that m increases with the increase in both roughness and stability. For example, for a moderately rough surface with $m = 0.2$ under near-neutral stability conditions, it can be shown from Equation (11.15) that the exponent would be reduced to about 0.1 under very unstable conditions and increased to about 0.6 under very stable ($z_r/L = 1$) conditions.

11.4 Drag and Heat Transfer Relations

The surface stress and sensible heat flux are usually expressed or parameterized in terms of the bulk drag and heat transfer relations

$$\begin{aligned} \tau_0 &= \rho C_D U_r^2 \\ H_0 &= -\rho c_p C_H U_r(\Theta_r - \Theta_0) \end{aligned} \tag{11.16}$$

in which C_D and C_H are the drag and heat transfer coefficients, respectively, and U_r and Θ_r are the mean wind speed and potential temperature at the reference measurement height z_r. When z_r falls within the surface layer, it is easy to show from Equations (11.12) and (11.16) that

$$\begin{aligned} C_D &= k^2[\ln(z_r/z_0) - \psi_m(z_r/L)]^{-2} \\ C_H &= k^2[\ln(z_r/z_0) - \psi_m(z_r/z_0)]^{-1}[\ln(z_r/z_0) - \psi_h(z_r/L)]^{-1} \end{aligned} \tag{11.17}$$

Thus, according to the Monin–Obukhov similarity theory, the drag and heat transfer coefficients are some universal functions of z_r/z_0 and z_r/L. Because the latter parameter involves the difficult-to-determine Obukhov length L, it should be useful and desirable to relate z_r/L to a more easily estimated parameter from

the known variables, U_r, Θ_r, Θ_0, and z_r. One such parameter is the bulk Richardson number

$$\mathrm{Ri_B} = (g/T_0)[(\Theta_r - \Theta_0)z_r/U_r^2] \tag{11.18}$$

Which can be related to z_r/L by substituting into Equation (11.18) from the M–O profile relations given by Equation (11.12). It is easy to show that

$$\mathrm{Ri_B} = \frac{z_r}{L}\left[\ln\frac{z_r}{z_0} - \psi_h\left(\frac{z_r}{L}\right)\right]\left[\ln\frac{z_r}{z_0} - \psi_m\left(\frac{z_r}{L}\right)\right]^{-2} \tag{11.19}$$

which is of the form $\mathrm{Ri_B} = F(z_r/z_0, z_r/L)$. The inverse of this function can be used to determine z_r/L for given values of z_r/z_0 and $\mathrm{Ri_B}$. For this a graphical representation of Equation (11.19) would be useful.

Knowing the general forms of ψ functions one can infer from Equation (11.17) that both the drag and heat transfer coefficients increase with increasing surface roughness (decreasing z_r/z_0) and decrease with increasing stability (see Figure 11.6). Their typical values over comparatively smooth water surfaces range from 1.0×10^{-3} to 2×10^{-3}. For land surfaces, however, the range of

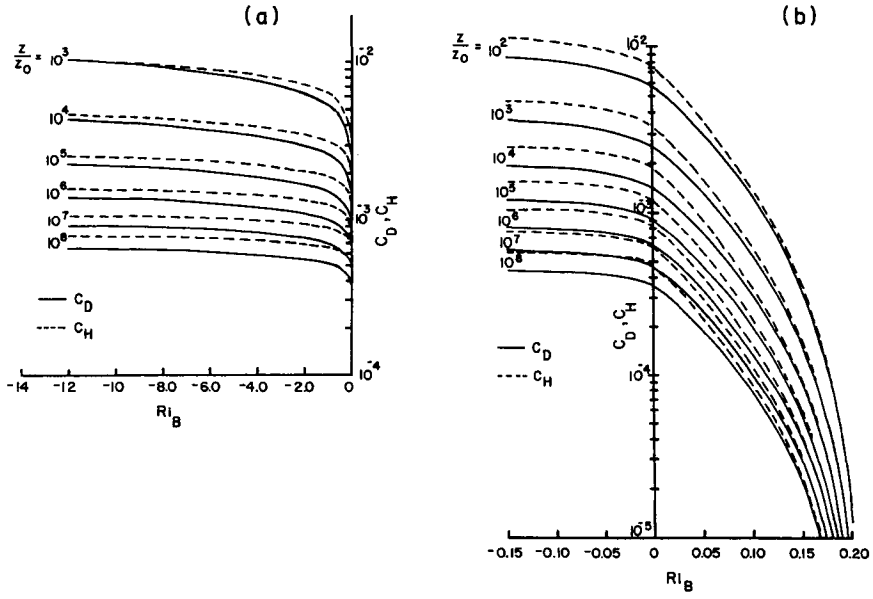

Figure 11.6 Variation of surface drag and heat transfer coefficients with surface roughness and the bulk Richardson number for (a) unstable conditions, and (b) near-neutral and stable conditions. [After Arya (1977).]

C_D and C_H values is considerably wider (say, 0 to 0.01). These are only weakly dependent on the choice of observation level in the surface layer; the most frequently recommended observation height for surface meteorological observations is 10 m.

11.5 Methods of Determining Momentum and Heat Fluxes

Determination of turbulent exchanges taking place between the earth and the atmosphere near their interface (surface) is of primary concern in micrometeorology. A number of methods have been devised with varying degrees of sophistication, some of which will be described here only briefly. The emphasis here is on principles and techniques, rather than on the details of instrumentation and measurements (Lenschow, 1986).

11.5.1 Surface-drag measurements

The only direct method of measuring shearing stress on a small sample of the surface is through the use of a carefully installed drag plate. The drag measured on the sample surface (plate) area must be representative of the whole area under consideration. This presumes a reasonably uniform ground cover with small roughness elements, which remain relatively undisturbed by the installation of the drag plate. The original roughness characteristics of the surface are retained or duplicated on the top of the drag plate. The drag plate has a small annular ring around it to isolate it from the surrounding area for drag force measurements using strain gauges and electromechanical transducers. The installation and successful operation of a drag plate requires considerable care, skill, and experience (Bradley, 1968). For this reason, such measurements have been made only in the context of a few micrometeorological experiments or research expeditions (e.g., the 1968 Kansas Field Program).

11.5.2 Energy balance method

No method exists for directly measuring the surface heat flux. A thin heat flux plate of known conductivity, with an embedded thermopile to measure temperature gradient across the plate, is often used to measure heat flux through the subsurface medium (e.g., soil, ice, and snow). But, to avoid radiative and convective effects the plate must be buried at least 10 mm below the surface. One can determine the ground heat flux H_G after applying an appropriate correction to the heat flux plate measurements. The sensible heat flux at the surface to or

from air can be estimated indirectly, using the surface energy balance or other appropriate energy budget equation discussed in Chapter 2, provided other components of the energy balance are measured or can otherwise be estimated. The energy balance method is often used in conjunction with the estimated Bowen ratio from mean temperature and humidity measurements at two heights near the surface.

11.5.3 Eddy correlation method

The most reliable and direct measurements of turbulent exchanges of momentum and heat in the atmosphere are usually made with sophisticated fast-response turbulence instrumentation. If all fluctuations of velocity and temperature that contribute to the desired momentum and heat fluxes are faithfully sensed and recorded, one can determine their covariances simply by averaging the products of the appropriate fluctuations over any desired averaging time. In particular, the vertical fluxes of momentum and heat over a homogeneous surface are given by

$$\begin{aligned} \tau &= -\rho\overline{uw} \\ H &= \rho c_p \overline{\theta w} \end{aligned} \tag{11.20}$$

with the x axis oriented along the mean wind. Because the above fluxes are expected to remain constant, independent of height, in a horizontally homogeneous surface layer eddy correlation measurements also provide a means of determining the surface fluxes ($\tau_0 \cong -\rho\overline{uw}$ and $H_0 \cong \rho c_p \overline{\theta w}$).

Although the eddy correlation method of determining fluxes is simple, in practice, it requires expensive research-grade instrumentation, such as sonic, laser, or hot-wire anemometers and thin-wire resistance thermometers, as well as rapid (sampling rates of 10–100 s^{-1}) data acquisition systems. The closer to the surface the turbulence measurements are made, the more severe become the instrument response problems. At heights greater than 10 m or so, light cup, vane, and propeller anemometers may also be adequate for measuring variances and fluxes. Larger averaging times may be required, however, with increasing height of measurement, because the characteristic size of large eddies usually increases with height in the PBL. The requirements of instrument leveling, orientation, calibration, and maintenance are also quite severe for accurate eddy correlation measurements (Lenschow, 1986).

The above-mentioned instrumental requirements have kept the eddy correlation method from being widely used, except in special research expeditions. But, continued advances in instruments and data processing have already

resulted in their increased use for many applications. The method has the advantage of measuring turbulent exchanges directly, without too many restrictive assumptions about the nature of the surface (such as uniform, flat, and homogeneous) or of the atmosphere. It is the only method available for measuring turbulent fluxes inside plant canopies, or in the wakes of hills and buildings.

11.5.4 Bulk transfer method

Indirect methods of estimating fluxes from more easily measured mean winds and temperatures in the surface layer or the whole PBL are based on the appropriate flux-profile relations. The simplest and the most widely used method is the bulk aerodynamic approach, which is based on the bulk transfer formulas [Equation (11.16)]. This method can be used when measurements or computations (e.g., in a numerical model) of mean velocity and temperature are available only at one level, in conjunction with the desired surface properties (e.g., the surface roughness and temperature). If the observation height is low enough for it to fall in the surface layer, the appropriate drag and heat transfer coefficients in Equation (11.16) can be parameterized on the basis of the Monin–Obukhov similarity relations [Equation (11.17)], as described in Section 11.4. This will indeed be the case for most routine surface meteorological observations over land and ocean areas. On the other hand, if the observation level is near the top of the PBL, or the reference wind is geostrophic, C_D and C_H may be parameterized on the basis of the PBL similarity theory (Deardorff 1972b; Arya, 1984). In practice C_D and C_H over ocean surfaces are usually prescribed some constant average values (e.g., $C_D \cong C_H \cong 1.5 \times 10^{-3}$) derived from major marine meteorological experiments. Over land areas, C_D and C_H are found to vary over a much greater range, due to the effects of surface roughness and stability, but in many applications constant values are still prescribed for the sake of simplicity. It is not difficult, however, to incorporate in such parameterizations the stability-dependent correction factors, such as C_D/C_{DN} and C_H/C_{HN} as functions Ri_B (Deardorff, 1968), where C_{DN} and C_{HN} are the prescribed coefficients for neutral stability.

11.5.5 Gradient method

In order to use the bulk transfer method described above, one needs to know the surface roughness and the surface temperature. Such information is not always easy to come by. In fact, for very rough and uneven surfaces, the surface itself is not well defined and its temperature cannot be measured directly. This difficulty

can be avoided by making measurements at two or more heights in the surface layer. Here, we describe a simple gradient or aerodynamic method of determining fluxes from measurements of mean differences or gradients of velocity and temperature between any two heights z_1 and z_2 within the surface layer, but well above the tops of roughness elements.

The two most commonly used finite-difference approximations for the vertical gradient of a mean micrometeorological variable M are:

(1) Linear approximation

$$\left(\frac{\partial M}{\partial z}\right)_{z_a} \cong \frac{\Delta M}{\Delta z} = \frac{M_2 - M_1}{z_2 - z_1} \tag{11.21}$$

which is applicable at the arithmetic mean height $z_a = (z_1 + z_2)/2$.

(2) Logarithmic approximation

$$\left(\frac{\partial M}{\partial \ln z}\right)_{z_m} \cong \frac{\Delta M}{\Delta \ln z} = \frac{M_2 - M_1}{\ln(z_2/z_1)} \tag{11.22}$$

or

$$\left(\frac{\partial M}{\partial z}\right)_{z_m} \cong \frac{\Delta M}{z_m \ln(z_2/z_1)} \tag{11.23}$$

which is applicable at the geometric mean height $z_m = (z_1 z_2)^{1/2}$.

Note that the above two approximations may not be directly compared as they pertain to vertical gradients at different heights. However, each of them is likely to have some error associated with it, because the actual profile of the mean variable may not be either linear or logarithmic in height between z_1 and z_2. The error might be expected to increase with increasing deviation of the profile from that assumed in the finite-difference approximation and also with the increasing height interval $z_2 - z_1$, or the ratio z_2/z_1 (Arya, 1991). A comparative assessment of finite-difference errors in the estimation of velocity and potential temperature gradients in the atmospheric surface layer shows that the logarithmic approximation is far superior to the linear approximation in near-neutral, unstable, and convective conditions (Arya, 1991). Therefore, the former is more widely used and often recommended in the micrometeorological literature. In very stable conditions, however, the linear approximation might be superior, because mean velocity and temperature profiles become more nearly linear, especially in the upper part of the surface layer. Still, the errors associated with the use of the logarithmic approximation are estimated to

remain small (< 8%) enough to be generally acceptable. In most applications of the gradient method, the same gradient approximation is used, irrespective of atmospheric stability.

Using the logarithmic finite difference approximation for both the velocity and potential temperature gradients, the gradient Richardson number at the geometric mean height z_m can be estimated as

$$\mathrm{Ri}_m = \frac{g}{T_0}\frac{\Delta\Theta z_m}{(\Delta U)^2}\ln\frac{z_2}{z_1} \tag{11.24}$$

Then, the corresponding value of the M–O stability parameter $\zeta_m = z_m/L$ can be determined from Equation (11.10)

$$\begin{aligned} &\zeta_m = \mathrm{Ri}_m, \quad \mathrm{Ri}_m < 0 \\ &\zeta_m = \mathrm{Ri}_m/(1 - 5\mathrm{Ri}_m), \quad \text{for } 0 \le \mathrm{Ri}_m < 0.2 \end{aligned} \tag{11.25}$$

Knowing ζ_m, the M–O similarity functions ϕ_m and ϕ_h can be evaluated from Equation (11.9) and, then, the friction velocity and temperature scales can be calculated from Equation (11.2) as

$$\begin{aligned} u_* &= k\Delta U \Big/ \left(\phi_m \ln\frac{z_2}{z_1}\right) \\ \theta_* &= k\Delta\Theta \Big/ \left(\phi_h \ln\frac{z_2}{z_1}\right) \end{aligned} \tag{11.26}$$

The surface fluxes can be determined from the above estimated scales as $\tau_0 = \rho u_*^2$, and $H_0 = -\rho c_p u_* \theta_*$.

The finite-difference approximations [Equation (11.22)] may not be good enough when the ratio z_2/z_1 becomes very large. On the other hand, if the two height levels are too close to each other, the differences in velocities and temperatures at the two levels may not be well resolved. A good compromise is to specify the measurement heights such that $z_2/z_1 = 2$ to 4. Still, there must be expected some errors in the measurements of ΔU and $\Delta\Theta$, as well as in the estimation of $\partial U/\partial z$, $\partial\Theta/\partial z$, and Ri_m. These, in conjunction with uncertainties in the M–O flux-profile relations, may lead to errors of more than 20% in the estimates of surface fluxes. Due to the above-mentioned errors and other reasons, the estimated value of Ri_m in stably stratified conditions may even turn out to be greater than the critical value of 0.2. The gradient method becomes invalid and should not be used in such cases, unless more appropriate

forms of the M–O similarity functions for very stable conditions are used for this purpose.

Example Problem 1

The following measurements were made of the hourly-averaged wind speed and temperature at a homogeneous rural site:

z (m)	U (m s^{-1})	T (°C)
2	3.34	29.04
8	3.98	28.10

Using the gradient method, estimate the following:

(a) Velocity and potential temperature gradients at 4 m.
(b) The gradient Richardson number at 4 m and the Obukhov length.
(c) The friction velocity, temperature scale, and the surface heat flux.

Solution:

(a) Using the logarithmic finite-difference approximation, the velocity and temperature gradients at $z_m = \sqrt{z_1 z_2} = 4$ m are

$$\frac{\partial U}{\partial z} = \frac{1}{z_m}\frac{\Delta U}{\ln(z_2/z_1)} = \frac{0.64}{4\ln 4} = 0.115 \text{ s}^{-1}$$

$$\frac{\partial T}{\partial z} = \frac{1}{z_m}\frac{\Delta T}{\ln(z_2/z_1)} = -\frac{0.94}{4\ln 4} = -0.170 \text{ K m}^{-1}$$

$$\frac{\partial \Theta}{\partial z} \cong \frac{\partial T}{\partial z} + \Gamma = -0.170 + 0.01 = -0.16 \text{ K m}^{-1}$$

(b)
$$\text{Ri}_4 = \frac{g}{T_0}\frac{\partial\Theta/\partial z}{(\partial U/\partial z)^2} = -\frac{9.81 \times 0.16}{302.2 \times 0.0132} = -0.387$$

$$\frac{z_m}{L} = \text{Ri}_4 = -0.387$$

$$L = -\frac{4}{0.387} = -10.33 \text{ m}$$

(c) At $\zeta_m = -0.387$, the M–O similarity functions can be estimated as

$$\phi_m = (1 - 15\zeta_m)^{-1/4} \cong 0.619$$
$$\phi_h = (1 - 15\zeta_m)^{-1/2} \cong 0.383$$

Then, from Equation (11.26)

$$u_* = \frac{0.4 \times 0.64}{0.619 \times 1.386} = 0.298 \text{ m s}^{-1}$$

$$\theta_* = \frac{0.4 \times 0.92}{0.383 \times 1.386} = -0.693 \text{ K}$$

$$H_0 = -\rho c_p u_* \theta_* \cong 248 \text{ W m}^{-2}$$

11.5.6 Profile method

In order to minimize errors in the estimated fluxes, it is highly desirable to make measurements of mean velocity and temperature at several (more than two) levels within the surface layer. A good procedure for determining fluxes from such profile measurements is to fit the appropriate flux-profile relations to the observations, using the least-square technique. In this way, the effect of random experimental errors on flux estimates can be minimized. A simple graphical procedure can also be used for the same purpose, which is described here in the following.

First, calculate Ri from measurements of U and Θ at each pair of consecutive levels and obtain the best estimate of the Obukhov length L by fitting a straight line through the data points of z_m versus Ri plot for unstable conditions, or z_m versus $\text{Ri}/(1 - 5\text{Ri})$ plot for stable conditions. Note that in either case, according to Equation (11.25), the slope of the best-fitted line will be L. The second step is to plot U versus $\ln z - \psi_m(z/L)$ and Θ versus $\ln z - \psi_h(z/L)$ and draw best-fitted straight lines through these data points (see Figures 11.7 and 11.8). Note that the slopes of these lines, according to Equation (11.12), must be, k/u_* and k/θ_*, respectively, which readily determine u_*, θ_* and the surface fluxes. The additional information on intercepts can be used to determine z_0 and Θ_0 if desired. This follows from writing Equation (11.12) in the form

$$\begin{aligned} \ln z - \psi_m(z/L) &= \frac{k}{u_*} U + \ln z_0 \\ \ln z - \psi_h(z/L) &= \frac{k}{\theta_*} \Theta - \frac{k}{\theta_*} \Theta_0 + \ln z_0 \end{aligned} \tag{11.27}$$

Note that for a fixed value of $\ln z - \psi_m$ and $\ln z - \psi_h$, the values of U and Θ can be determined from the best-fitted lines through the data points, from which $\ln z_0$ and Θ_0 can be estimated, knowing k/u_* and k/θ_* from the slopes of the best-fitted lines.

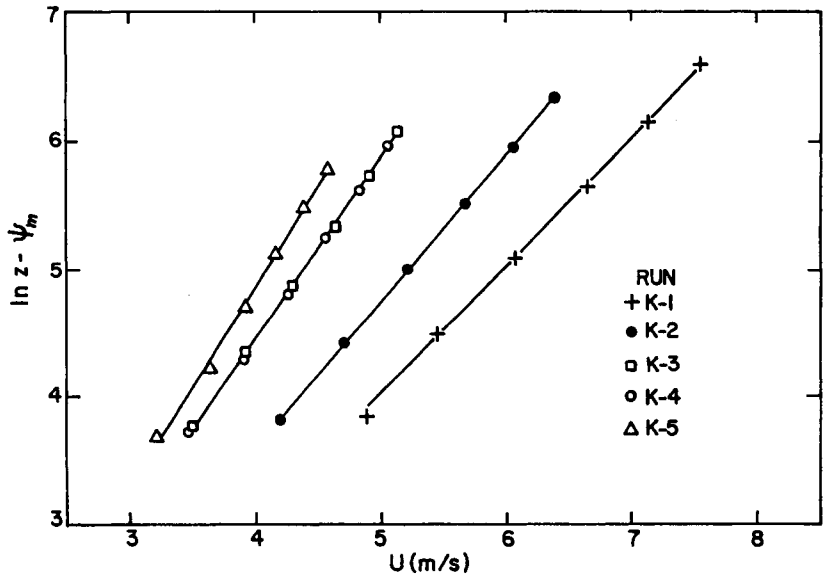

Figure 11.7 Least-square fitting of the M–O flux-profile relation (modified log law) to the observed mean velocity profiles at Kerang, Australia. [After Paulson (1967).]

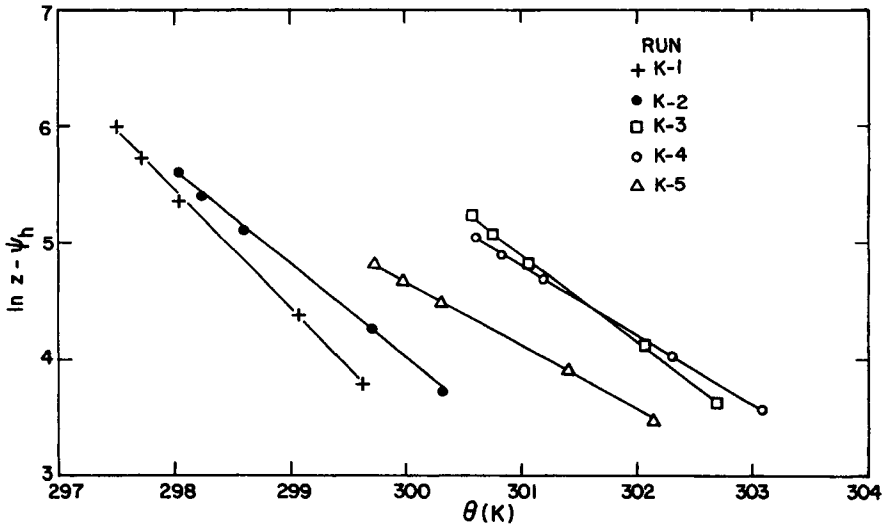

Figure 11.8 Least-square fitting of the M–O flux-profile relation (modified log law) to the observed mean potential temperature profiles at Kerang, Australia. [After Paulson (1967).]

The above procedure is an extension of the more familiar graphical method of determining the friction velocity or the surface stress from the observed wind profile in a neutral surface layer (see Chapter 10). The stability correction is made here to obtain a modified height coordinate in which the wind and potential temperature profiles are expected to be linear. If the surface roughness parameter is known or can be estimated, one can use a simpler version of the profile method that requires minimal measurements of wind speed at one level and temperatures at two height levels in the surface layer (Arya, 1999, Chapter 4).

11.5.7 Geostrophic departure method

The equations of mean motion (Chapter 9), with certain assumptions, can be used to determine the surface stress, as well as the profiles of turbulent momentum fluxes in the PBL. Here, we demonstrate this method for a horizontally homogeneous and quasistationary PBL for which the mean flow equations reduce to Equation (9.9). Their integration with respect to height from some level z to the top of the PBL, where the turbulent fluxes may be expected to vanish, gives momentum fluxes as functions of the height z

$$\begin{aligned} \overline{uw} &= -f\int_z^h (V - V_g)dz \\ \overline{vw} &= f\int_z^h (U - U_g)dz \end{aligned} \tag{11.28}$$

In particular, the surface stress is given by

$$\tau_0 = \rho f\int_0^h (V - V_g)dz \tag{11.29}$$

where the x axis is taken parallel to the surface wind or stress (this implies that $\overline{vw} = 0$ at $z = 0$, so that from Equation (11.28), $\int_0^h (U - U_g)dz = 0$ constitutes an integral constraint on the U profile]. The above relations are, of course, restricted to steady-state flow with no advection, but can easily be modified to include acceleration terms.

Note that Equations (11.28) and (11.29) express the local momentum fluxes and the surface stress in terms of the integrated departures of the actual wind components from the geostrophic wind components. Hence, the name 'geostrophic departure method' is given to this simple technique of determining

turbulent fluxes from more easily measured wind profiles (e.g., from pibals, rawinsondes, or remote-sensing wind profilers). The presence of accelerations, and uncertainties in the determination of actual mean winds, geostrophic winds, and the PBL height, frequently lead to deviations from the ideal case and, hence, to large errors in flux determinations. Because the top of the PBL where turbulent momentum fluxes are expected to vanish may not be easy to identify from mean wind profiles alone, the upper limit of integrals in Equations (11.28) and (11.29) is sometimes replaced by the heights z_u and z_v, where the U and V profiles have a maximum or minimum, provided such maxima or minima exist. This is based on the assumption, implied by the gradient-transport hypothesis, that $\overline{uw}$ and $\overline{vw}$ must vanish at the levels where $\partial U/\partial z$ and $\partial V/\partial z$ respectively become zero.

11.5.8 Thermodynamic energy equation method

A similar method for determining the sensible heat flux at the surface and its vertical distribution (profile) in the PBL is based on the thermodynamic energy equation which, in the absence of temperature advection, reduces to

$$\frac{\partial T}{\partial t} = \frac{1}{\rho c_p}\frac{\partial R_N}{\partial z} - \frac{\partial \overline{w\theta}}{\partial z} \tag{11.30}$$

Note that the time-tendency (warming or cooling rate) term is retained here, because it is often found to be significant even when the flow field may be considered quasistationary. It is a manifestation of the diurnal heating and cooling cycle which is responsible for important stability and buoyancy effects in the PBL. According to Equation (11.30), the rate of warming or cooling essentially balances the convergence or divergence of radiative and sensible heat fluxes. The radiative flux divergence is usually ignored in the daytime unstable or convective PBL, especially in the absence of fog and clouds within the layer. It becomes more significant in the stably stratified nocturnal boundary layer.

In simpler situations, where the radiative flux divergence can be ignored, the integration of Equation (11.30) with respect to height yields

$$\begin{aligned} \overline{w\theta} &= \int_z^h \frac{\partial T}{\partial t} dz \\ H_0 &= \rho c_p \int_0^h \frac{\partial T}{\partial t} dz = \rho c_p h \left(\frac{\partial T}{\partial t}\right)_m \end{aligned} \tag{11.31}$$

where $(\partial T/\partial z)_m$ denotes the mean rate of warming in the PBL and we have assumed that the sensible heat flux vanishes at the top of the PBL, i.e., at $z = h$, $\overline{w\theta} = 0$. Thus, temperature soundings in the PBL at close intervals (say 1–3 h) may be used with Equation (11.31) to determine H_0 and the $\overline{w\theta}$ profile. Alternatively, the rate of warming can be estimated from continuous temperature measurements at a height above which the rate of warming becomes almost independent of height in the PBL. This is usually the case in the unstable or convective mixed layer at $z \geq 50$ m. However, the rate of warming at the standard reference height of 10 m may not be significantly different from that in the mixed layer, so that the former may provide a good approximation for $(\partial T/\partial t)_m$. One still needs an estimate of the PBL height h, either from a sounding or from an appropriate model or parameterization of h (Stull, 1988; Arya, 1999).

Both the geostrophic departure and thermodynamic energy methods are quite useful and reliable in that these are based on the fundamental conservation equations and measurements of mean wind and temperature profiles, without any restrictive assumptions, as implied in the empirical flux-profile relations. The simplifying assumptions of steady state and no advection can be relaxed whenever they cannot be justified and advection/acceleration terms can be evaluated from mean profile measurements.

11.5.9 Variance method

In a horizontally homogeneous and quasistationary PBL the turbulent fluxes or covariances are intimately related to the variances or standard deviations of velocity and temperature fluctuations through the various similarity relations for turbulence structure. Since variances can be measured more easily and accurately than covariances or turbulent fluxes, the latter may be determined indirectly by measuring the former and using the appropriate similarity relations. Fast-response instruments are required, which is a disadvantage in comparison with other indirect methods requiring measurements of mean winds and temperatures. However, the fact that observations at a single level may yield momentum and heat fluxes is an added attraction of the variance method.

The method is best suited for determining the surface fluxes from measurements of σ_w and σ_θ at an appropriate level (say, 10 m) in the fully developed surface layer, because the similarity relations are simpler and well established for a wide range of surface types and stability conditions. For example, in the unstable surface layer both σ_w and σ_θ follow the local free convection similarity relations [Equation (9.41)] (see Figure 11.9), either of which can be used to determine the surface heat flux. In the stably stratified surface layer, on the other hand, the local similarity scaling of turbulence structure implies that the ratios

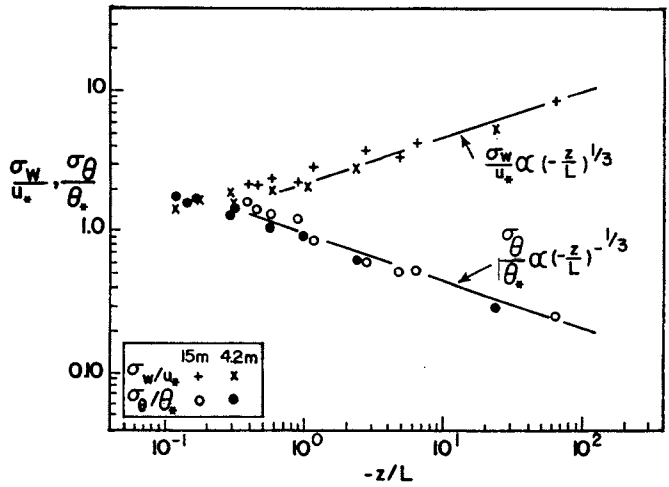

Figure 11.9 Normalized standard deviations of vertical velocity and temperature fluctuations as functions of $-z/L$, compared with local free convection similarity relations. [From Businger (1973); after Monji (1972).]

σ_w/u_* and σ_θ/θ_* must be constants, independent of height, where $u_* = (-\overline{uw})^{1/2}$ and $\theta_* = -\overline{w\theta}/u_*$. This can be used to estimate the local fluxes from measurements of σ_w and σ_θ. In slightly unstable to slightly stable conditions, the Monin–Obukhov similarity theory predicts σ_w/u_* and σ_θ/θ_* to be some unique functions of z/L, which have been evaluated on the basis of micrometeorological data from homogeneous sites. In particular, the empirical formula

$$\frac{\sigma_w}{u_*} = 1.25[1 - 3(z/L)]^{1/3} \tag{11.32}$$

obtained from a compilation of many aircraft and tower data taken over land and sea surfaces can be recommended for unstable conditions (see also Panofsky and Dutton, 1984, Chapter 7). A plot of Equation (11.32) with the experimental data on σ_w/u_* as a function of $-z/L$ is shown in Figure 11.10.

The surface heat flux in a convective boundary layer (CBL) can also be estimated from measurements of σ_u or σ_v at any convenient height in the lower part of the CBL where the empirical similarity relations $\sigma_u \cong \sigma_v \cong 0.6W_*$ are found to be valid (Caughey and Palmer, 1979). Since, the convective velocity scale W_* is related to the mixed-layer height and the surface heat flux, the latter can be estimated if the mixed-layer height is measured independently (e.g., from temperature sounding).

In some applications, the above-mentioned similarity relations between the turbulent fluxes and variances are used to determine the latter from indirect

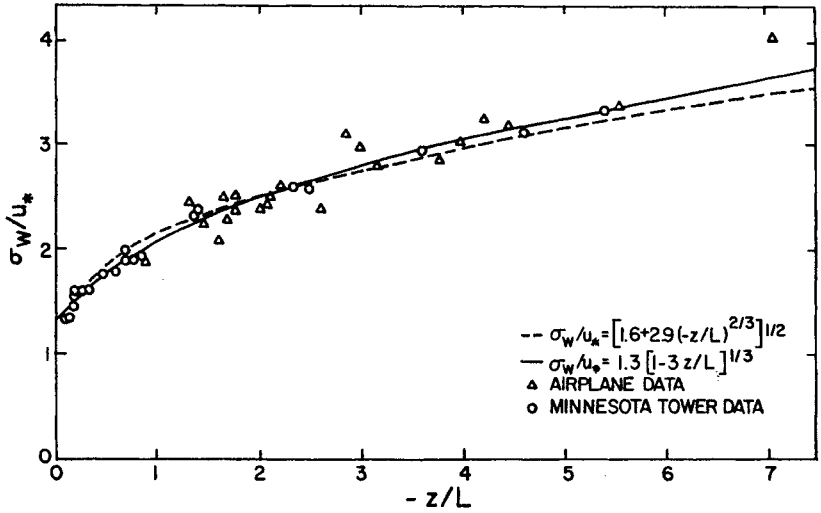

Figure 11.10 Normalized standard deviation of vertical velocity fluctuations in the surface layer as a function of z/L. [After Panofsky *et al.* (1977).]

estimates of the former. For example, the horizontal and vertical spread of a chimney plume or a pollutant cloud is intimately related to velocity variances, which need to be indirectly estimated in the absence of turbulence measurements.

Example Problem 2

The following measurements were made at a suburban site during the afternoon (say, at 2:00 PM) convective conditions:

Mean temperature at 10 m height = 17.0°C.

Average rate of warming at 10 m = 0.60 K h^{-1}.

Mixing height from the temperature sounding = 1500 m.

Using the appropriate thermodynamic and similarity relations, estimate the following at the time of above measurements:

(a) The surface heat flux.

(b) σ_u, σ_v, and σ_w at 10 m and 100 m heights.

Solution

(a) Assuming that the rate of warming at 10 m is representative of that in the whole convective boundary layer, we can use Equation (11.31) to estimate the surface heat flux as

$$H_0 = \rho c_p h \left(\frac{\partial T}{\partial t}\right)_m = \frac{1200 \times 1500 \times 0.6}{3600} = 300 \text{ W m}^{-2}$$

(b) $\sigma_u = \sigma_v \cong 0.6W_*$, which is independent of height, where

$$W_* = \left(\frac{g}{T_0}\frac{H}{\rho c_p}h\right)^{1/3} = \left(\frac{9.81}{290} \times \frac{300}{1200} \times 1500\right)^{1/3} = 2.31 \text{ m s}^{-1}$$

Thus, $\sigma_u = \sigma_v \cong 1.39$ m s^{-1} at both the 10 m and 100 m heights.
For estimating σ_w in the convective surface layer, the local free convection similarity relation (9.41) is more appropriate, so that

$$\sigma_w = 1.4\left(\frac{g}{T_0}\frac{H_0}{\rho c_p}z\right)^{1/3}$$

From this we can estimate $\sigma_w = 0.61$ and 1.31 m s^{-1} at the 10 m and 100 m heights, respectively.

11.6 Applications

Theory and observations of momentum and heat exchanges between the atmosphere and the earth's surface, presented in this chapter, may have the following practical applications:

- Systematic ordering of mean wind, temperature, and turbulence data with stability in the surface layer.
- Quantitative description of the surface layer wind and temperature profiles and their relationship to the surface fluxes of momentum and heat.
- Specifying eddy diffusivities and bulk transfer coefficients as functions of stability in the parameterizations of fluxes.
- Determining surface and PBL fluxes from different types of mean flow and turbulence measurements.
- Parameterizing turbulence and diffusion in the atmospheric surface layer.
- Determining the surface energy budget.

Problems and Exercises

1. What maximum error or uncertainty might be expected in the determination of the Obukhov length, if the fluxes of the momentum and heat have uncertainties of $\pm 20\%$ associated with them?

2. Using the definitions of the various scales and parameters and the basic

Monin–Obukhov similarity relations [Equation (11.2)], verify or derive Equations (11.4) and (11.5).

3. Using the similarity functions obtained by Businger *et al.* (1971) from the 1968 Kansas Field Program, calculate and plot the Richardson number as a function of z/L in the range $-2 \leq z/L \leq 2$, and compare it with the graph based on the simpler relations [Equation (11.10)]. What conclusions can you draw from this?

4. Substituting from the M–O similarity profile relations in the bulk transfer formulas [Equation (11.16)],

(a) derive the expressions given by Equation (11.17) for C_D and C_H as functions of z/L and z/z_0;

(b) write the same as functions of the bulk Richardson number $\mathrm{Ri_B}$ for stable conditions ($\mathrm{Ri_B} > 0$), and plot C_D/C_{DN} as a function of $\mathrm{Ri_B}$ for $z_r/z_0 = 10^3$ and 10^6.

What conclusions can you draw from this?

5. The following measurements of mean wind and potential temperature were taken around noon during the 1968 Kansas Field Program:

z (m)	2	4	8	16	32
U (m s^{-1})	5.81	6.70	7.49	8.14	8.66
Θ (K)	307.20	306.65	306.28	305.88	305.62

Using the M–O similarity relations $\phi_h = \phi_m^2 = [1 - 15(z/L)]^{-1/2}$ for the unstable surface layer.

(a) Calculate and plot Ri as a function of height.

(b) Determine the Obukhov length from the above plot.

(c) Calculate the surface shear stress τ_0 and the heat flux H_0, using the gradient method with the data from the lowest two (2 and 4 m) heights; take $\rho = 1.2$ kg m^{-3} and $c_p = 10^3$ J kg^{-1} K^{-1}.

6. The following observations were taken on a summer evening during the Kansas Experiment (with a surface pressure of 1000 mbar):

z (m)	2	4	8	16
U (m s^{-1})	2.84	3.39	4.01	4.85
T (°C)	33.09	33.31	33.57	33.82

(a) Use the graphical version of the profile method discussed in the text to determine u_* and θ_*.
(b) Use the gradient method for the same purpose, using information from the lowest two (2 and 4 m) heights only.
(c) Compare the results of the above two methods with the eddy correlation measurements of $\overline{uw} = -0.044\ \text{m}^2\ \text{s}^{-2}$ and $\overline{w\theta} = -0.023\ \text{m s}^{-1}\ \text{K}$.

7. During the Minnesota 1973 Experiment, the following mean temperature measurements were made from a tethered balloon at 75 min intervals:

	T (°C)	
z (m)	1217–1332 (CDT)	1332–1447 (CDT)
2	21.75	22.46
61	19.54	20.25
305	17.16	17.86
610	14.43	15.16
914	11.66	12.34
1219	8.99	9.61

(a) Calculate the warming rate at various levels and the average value for the whole PBL. What conclusion can you draw on the variation of the rate of warming with height?
(b) Calculate the surface heat flux in the middle of the observation period when the PBL height was 1400 m, assuming a constant (average) warming rate, independent of height. Compare this with the direct (eddy correlation) measurement of $\overline{w\theta} = 0.20\ \text{m s}^{-1}\ \text{K}$.
(c) Suggest a simpler method of estimating the surface heat flux in daytime, using temperature measurements at only one level and remote sensing of the PBL height from the surface.